Yunfei Xu
Department of Mechanical Engineering,
Michigan State University
e-mail: xuyunfei@egr.msu.edu

Jongeun Choi[1]
Department of Mechanical Engineering,
and Department of Electrical and Computer Engineering,
Michigan State University,
2459 Engineering Building,
East Lansing, MI 48824-1226
e-mail: jchoi@egr.msu.edu

N. Peter Reeves
e-mail: reevesn@msu.edu

Jacek Cholewicki
e-mail: cholewic@msu.edu

Department of Surgical Specialties,
Michigan State University

Optimal Control of the Spine System

The goal of this work is to present methodology to first evaluate the performance of an in vivo spine system and then to synthesize optimal neuromuscular control for rehabilitation interventions. This is achieved (1) by determining control system parameters such as static feedback gains and delays from experimental data, (2) by synthesizing the optimal feedback gains to attenuate the effect of disturbances to the system using modern control theory, and (3) by evaluating the robustness of the optimized closed-loop system. We also apply these methods to a postural control task, with two different control strategies, and evaluate the robustness of the spine system with respect to longer latencies found in the low back pain population. This framework could be used for rehabilitation design. To this end, we discuss several future research needs necessary to implement our framework in practice. [DOI: 10.1115/1.4000955]

1 Introduction

Classic studies investigating spinal stability have documented that the critical load that the osteoligamentous spine (spine devoid of muscles) can bear before buckling is approximately 90 N or 20 lbs [1]. Given that the upper body mass exceeds this critical threshold, it can be shown that the in vivo human lumbar spine is unstable. Therefore, some form of control must be applied to give it stable behavior [2]. For any given task, there exist various control strategies that will ensure a stable spine. Consequently, the central nervous system (CNS) has some flexibility when choosing a suitable control scheme and may emphasize one that stresses performance over reducing metabolic costs or vice versa.

There is growing evidence that people with low back pain (LBP) have different control strategies than healthy individuals. Several studies have reported higher levels of trunk muscle coactivation associated with LBP [3–5], which may reflect a protective coping strategy. Recently, it has been shown that the introduction of pain from hypertonic saline injection into paraspinal muscles leads to altered muscle recruitment that is similar to that found in LBP [6]. Interestingly, when this painful stimulus was removed, muscle recruitment did not return to its original state, suggesting that even following recovery, the CNS may be confined to a protective coping strategy.

To determine if protective trunk coactivation can result in a functional impairment, we recorded postural sway during a seated balancing task [7]. This task emphasizes trunk muscle's contribution during postural control. Results from the study suggested that elevated trunk muscle coactivation resulted in impaired postural control. One explanation for this impairment is that coactivation results in higher gains in feedback control [8], which when coupled with delays in feedback loops impairs postural control. Pertinent to this hypothesis, several studies have found longer delays in reflex responses of trunk muscles in LBP patients compared with healthy individuals [9–12]. Furthermore, postural control experiments have shown that people with LBP have more postural sway than healthy individuals [13,14], and correlated increased postural sway with longer trunk muscle reflex latencies [15]. This evidence suggests that after a painful episode, individuals who continue with a protective coping strategy may be relying on a nonoptimal control scheme, one that may predispose them to re-injury and pain [16].

Using concepts and controller synthesis techniques from modern control theory [17–19], optimal control of the spine can be designed and used to guide neuromuscular retraining. This can be achieved by estimating and modeling force disturbances in muscles and noise in sensory circuits [20–23], and then designing the closed-loop spine system to minimize the effect of such disturbances by adjusting feedback gains [17]. In the process, feedback gains in a stable system can be optimized based on a performance-cost function. In addition, it is also possible to assess the robustness of the spine system to changes or uncertainty in the parameters of the system.

The goal of this work is to present methodology to first evaluate the performance of a spine system and then to synthesize optimal neuromuscular control for rehabilitation interventions. This is achieved (1) by determining control system parameters such as static feedback gains and delays from experimental data, (2) by synthesizing the optimal feedback gains to attenuate the effect of disturbances to the system using modern control theory [17] and numerically efficient convex optimization (or linear matrix inequalities (LMI)) techniques [18,19], and (3) by evaluating the robustness of the optimized closed-loop system. Given that this paper represents a generic framework for rehabilitation design, we plan to show how these methods could be applied to a postural control task, with two different control strategies (aimed at minimizing steady-state kinematic outputs and the control effort) and with evaluating the robustness of the spine system with respect to error in predicting trunk muscle reflex latencies.

This paper is organized as follows. In Sec. 2, we briefly review the postural task known as seated balancing, its model, and the experimental setup described in detail in Ref. [24]. The sensory noise and disturbance are also modeled. Section 3 introduces iterative optimization techniques for synthesizing way points of fixed-structure controllers for some $\mathcal{H}_2$ performance-cost func-

[1]Corresponding author.

Contributed by the Bioengineering Division of ASME for publication in the JOURNAL OF BIOMECHANICAL ENGINEERING. Manuscript received May 20, 2009; final manuscript received December 17, 2009; accepted manuscript posted January 6, 2010; published online March 25, 2010. Assoc. Editor: Noshir Langrana.

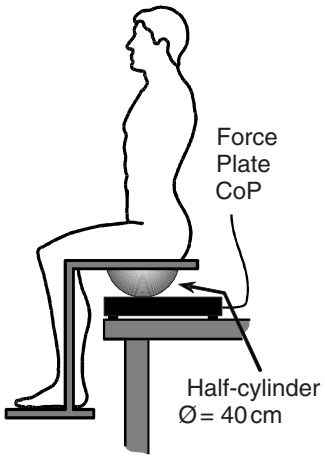

Fig. 1 A subject balancing on an unstable seat. The upper body angle and angular velocity (θ_1, $\dot{\theta}_1$) and the lower body (seat) angle and angular velocity (θ_2, $\dot{\theta}_2$) were collected during the experiment.

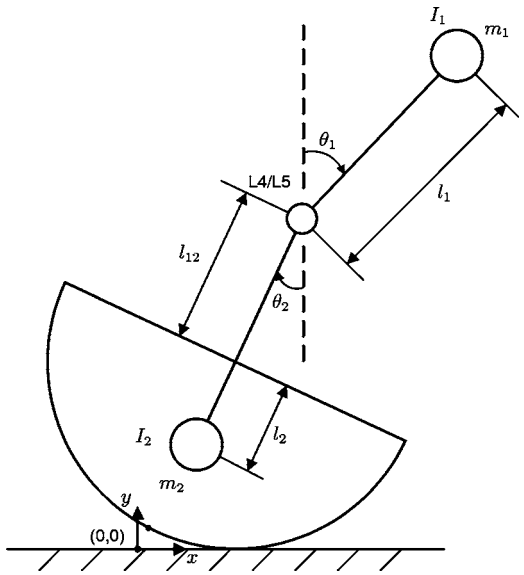

Fig. 2 The dynamic model of postural control during unstable sitting

tions. In Sec. 4, an illustrative case study of a subject is conducted and improved performances are analyzed. The robustness of the spine systems with respect to changes in time delays are discussed in Sec. 5. Section 6 discusses the application of these methods to LBP rehabilitation, including current limitations in knowledge requiring further research.

Standard notation is used throughout the paper. Let $\mathbb{R}$ denote the set of real numbers. The positive definiteness (and semidefiniteness) of a matrix A is denoted by $A>0$ (and $A\geqslant 0$, respectively). Other notation will be explained in due course.

2 The Unstable Seated Balance Task

In this paper, we consider postural control of a spine system during an unstable seated balance task. The seated balance task emphasizes trunk muscles' contribution in maintaining posture and thus provides a useful tool to evaluate trunk neuromuscular control. The feedback controller for the spine system consists of intrinsic properties of intervertebral joints (i.e., joint stiffness and damping) and trunk muscles (i.e., short range muscle stiffness and damping) and command signals from the CNS. Feedback control from intrinsic pathways is instantaneous, whereas feedback control from the CNS has inherent delays. These delays represent the time taken to sense a perturbation and respond with increased muscle activation to counteract the disturbance. In the presence of a disturbance, some or all of these feedback pathways can be utilized to provide the necessary and appropriate force to stabilize the spine.

The lumped spine model during the unstable sitting is based on the work of Reeves et al. [24]. Briefly, the seated balance system can be described by two second-order equations representing the equations of motion for the upper body mass (m_1) and the lower body mass (m_2) along with the torque actuator at L4/L5 representing muscle action, as shown in Figs. 1 and 2. The time series data of upper body angle θ_1 and lower body (seat) angle θ_2 were collected during the experiment using a motion capture system (Phoenix Technologies Inc., Burnaby, BC, Canada). Subjects were asked to lean against a cable attached to an electromagnet while balancing on the seat. At a random time interval, the electromagnet was deactivated, releasing the cable. Subjects' postural responses, representing the movement of the upper and lower bodies, were recorded following the release. The motion was constrained to the coronal plane by placing the seat on a half-cylindrical base. The goal of the task is to stabilize the posture so that state variables $\theta_1, \dot{\theta}_1, \theta_2, \dot{\theta}_2$ become zero. Using the lumped model shown in Fig. 2, the equations of motion have been derived based on Lagrangian mechanics [24]. The control input (neural excitation) applied to the model is based on proportional feedback gains for the four state variables passing through feedback delays, reflecting nonintrinsic contributions to neuromuscular control. The excitation-contraction (muscle actuator) dynamics [25] have been included in the model. The resulting model is a time-delayed nonlinear system. Using the equations of motion, we have identified subject specific control system parameters such as static feedback gains and delays from his/her experimental data [24]. In particular, control system parameters have been identified using nonlinear least-squares optimization to match model simulations to the experimental data. We have noticed that the experimentally observed state deviation is normally contained in a small neighborhood of the origin. Hence, for the controller synthesis purpose, we linearize the nonlinear dynamics and replace the time delays with the finite-order Padé approximation, which provides us the linear time-invariant (LTI) system.

We use the Padé approximation to replace time delays with rational LTI models

$$P_\tau(s) = \frac{(\tau s)^2 - 6(\tau s) + 12}{(\tau s)^2 + 6(\tau s) + 12} \approx e^{-\tau s}$$

Noise to each of sensory channels is modeled by the output of a linear system driven by Gaussian white noise

$$n_i(t) = \int_{-\infty}^{\infty} g_i(t-\tau)\tilde{n}_i(\tau)d\tau, \quad i = 1, \ldots, 4$$

where $\tilde{n}_i(t)$ is Gaussian white noise with a unit power spectral density (PSD) (i.e., $S_{\tilde{n}_i}(\omega)=1$). The Laplace transform of the impulse response g_i is given by

$$\mathcal{L}(g_i(t)) = W_{n_i}(s) = \frac{b_i}{a_i s + 1}$$

The resulting PSD and the variance of $n_i(t)$ are, respectively,

$$S_{n_i}(\omega) = |W_{n_i}(j\omega)|^2 S_{\tilde{n}_i}(\omega)$$

and

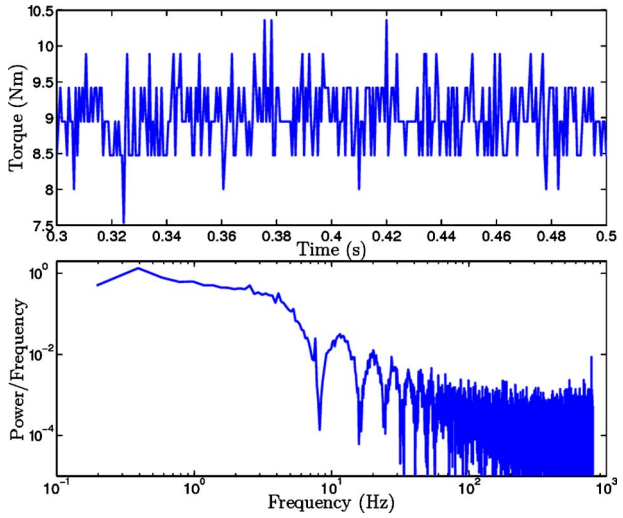

Fig. 3 The trunk torque disturbance measured at the 5% of the maximum voluntary effort and the associated power spectral density

$$\sigma^2 = \mathbb{E}\{|n_i(t)|^2\} = \frac{1}{2\pi}\int_{-\infty}^{\infty} |W_{n_i}(j\omega)|^2 d\omega$$

where $\mathbb{E}$ denotes the expectation operator. We have chosen parameters as follows. The standard deviation σ was adjusted to the experimentally evaluated motion perception threshold in Ref. [22], (i.e., 3σ=0.34 deg). The PSD of the sensory noise was selected as in Ref. [22]. Hence we obtain

$$W_{n_i}(s) = \frac{0.01}{10s+1} \tag{1}$$

indicating that most of the sensor noise energy is located at the low frequency range.

The torque disturbance is also obtained by filtering the unit Gaussian white noise with a low-pass filter $W_d(s)$ defined as

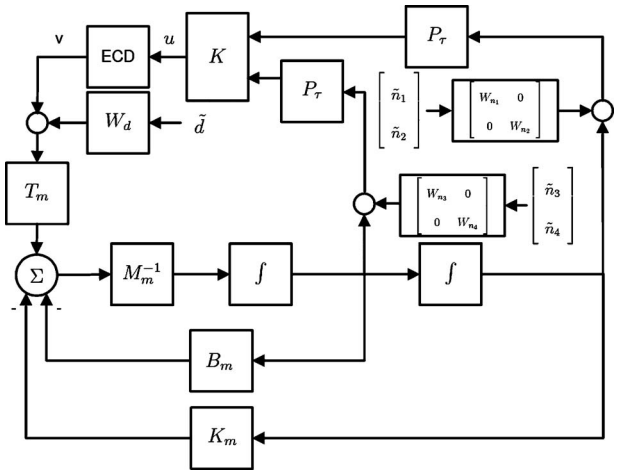

Fig. 4 The block diagram of the spine system. M_m, B_m, K_m, and T_m are matrices defined in Eq. (3). K is the feedback controller. ECD is the excitation-contraction dynamics. $\tilde{n}_i$ and $\tilde{d}$ are the sensor noise and the disturbance input, respectively. W_{n_i} and W_d are the sensor noise dynamics and the disturbance dynamic, respectively. P_τ is the approximated delay.

$$W_d(s) = \frac{0.1}{0.05s+1} \tag{2}$$

The bandwidth of the low-pass filter in Eq. (2) was chosen to match the PSD of the torque disturbance experimentally measured (Fig. 3). The resulting standard deviation of the torque disturbance was chosen to match the trunk torque variability at the 5% of the maximum voluntary effort documented in Ref. [21]. The detail of the experiment protocol is illustrated in Ref. [21].

3 Synthesis of the Optimal Controller

In this section, we present the design of optimal feedback gains with respect to a performance-cost function for the unstable seated balance task.

$$\underbrace{\begin{bmatrix} m_1 l_1^2 + I_1 & m_1 l_1 r + m_1 l_1 l_{12} \\ m_1 l_1 r + m_1 l_1 l_{12} & (m_1+m_2)r^2 + 2(m_1 - m_2) l_{12} r + m_1 l_{12}^2 + m_2 l_2^2 + I_2 \end{bmatrix}}_{=:M_m} \begin{bmatrix} \ddot{\theta}_1 \\ \ddot{\theta}_2 \end{bmatrix}$$
$$+ \underbrace{\begin{bmatrix} b & -b \\ -b & b \end{bmatrix}}_{=:B_m} \begin{bmatrix} \dot{\theta}_1 \\ \dot{\theta}_2 \end{bmatrix} + \underbrace{\begin{bmatrix} k - m_1 l_1 g & -k \\ -k & k - m_1 l_{12} g + m_2 l_2 g \end{bmatrix}}_{=:K_m} \begin{bmatrix} \theta_1 \\ \theta_2 \end{bmatrix} = \underbrace{\begin{bmatrix} -1 \\ 1 \end{bmatrix}}_{=:T_m} u \tag{3}$$

The linearized spine model with respect to the origin is provided in Eq. (3) in which the parameters are defined, as shown in Fig. 2. As illustrated in Fig. 4, the block diagram of the closed-loop spine system consists of the linearized lumped spine model, a feedback gain vector (K), excitation-contraction dynamics (ECD), sensor noise dynamics (W_{n_i}), disturbance dynamics (W_d), and approximated delays (P_τ).

The closed-loop system in Fig. 4 can be viewed as a generalized plant P and a controller K in Fig. 5:

$$\dot{x} = Ax + B_w w + B_u u$$

$$z = C_z x + D_{zu} u$$

$$y = C_y x$$

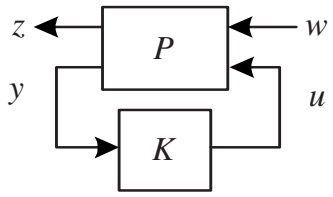

Fig. 5 The closed-loop system. *P* is the generalized plant and *K* is the controller.

$$u = Ky \tag{4}$$

where $x \in \mathbb{R}^n$ is the resulting state vector. $w := [\tilde{n}_1 \ \tilde{n}_2 \ \tilde{n}_3 \ \tilde{n}_4 \ \tilde{d}]^T \in \mathbb{R}^5$ is the disturbance. Since we use the sensor noise and disturbance dynamics, respectively, in Eqs. (1) and (2), $\{\tilde{n}_i(t) | i = 1, \ldots, 4\}$ and $\tilde{d}(t)$ are unit white noise random variables that generate the sensory noise and the torque disturbance. Hence, w is a white noise random vector with a unit covariance matrix satisfying

$$\mathbb{E}(w(t)) = 0 \in \mathbb{R}^5, \quad \mathbb{E}(w(t)w^T(t-\tau)) = \delta(\tau)I_5 \in \mathbb{R}^{5\times 5}$$

where $\delta(\cdot)$ is the Dirac delta function and I_n denotes the identity matrix of size n. We also define the pure performance output of the closed-loop system by

$$x_{1:4} := \begin{bmatrix} x_1 \\ x_2 \\ x_3 \\ x_4 \end{bmatrix} = \begin{bmatrix} \theta_1 \\ \theta_2 \\ \dot{\theta}_1 \\ \dot{\theta}_2 \end{bmatrix} \in \mathbb{R}^4$$

$u \in \mathbb{R}$ is the feedback control input. $z := [x_{1:4}^T \ ru_e]^T \in \mathbb{R}^5$ is the performance output including the error output $x_{1:4}$ as well as the weighted control effort u_e (i.e., the output of the excitation-contraction dynamics model) by a factor $r > 0$. $y \in \mathbb{R}^4$ is the noisy output measurement of $x_{1:4}$. A model of unstable seated balancing with a fixed-structure feedback controller reproduced experimental data very well [24]. The static control gain vector K is given by

$$K := \begin{bmatrix} k_1 & k_2 & k_3 & k_4 \end{bmatrix} \in \mathbb{R}^{1\times 4}$$

The closed-loop system is then given by

$$\begin{aligned} \dot{x} &= \underbrace{(A + B_u K C_y)}_{:=A_{cl}} x + B_w w \\ z &= \underbrace{(C_z + D_{zu} K C_y)}_{:=C_{cl}} x \end{aligned} \tag{5}$$

The goal of the feedback control is to stabilize the spine system so that $\|x_{1:4}\| \to 0$ and to minimize the effect of the disturbance w.

Notice that we need to design a fixed-structure feedback controller K [26–28] as compared with the standard optimal state (or output) feedback controller [17]. To obtain way points of controllers starting from the experimentally determined initial control gains to the optimal control gains continuously, we are interested in iterative optimization algorithms that provide monotonically decreasing performance-cost values. This will allow a clinician to select any set of gains from a way point look-up table as a target for the rehabilitation. Now we introduce several such control synthesis schemes.

In this paper, we mainly consider the $\mathcal{H}_2$ norm as our performance-cost function for the spine system. Assuming that K in Eq. (5) ensures that A_{cl} is stable in Eq. (5), the $\mathcal{H}_2$ norm of the transfer function T_{zw} from the disturbance input w to the performance output z is defined by

$$\|T_{zw}\|_2 := \sqrt{\frac{1}{2\pi}\int_{-\infty}^{\infty} \mathrm{tr}(T_{zw}(j\omega)^H T_{zw}(j\omega))d\omega}$$

where T^H denotes the conjugate transpose of a matrix T. When the system is driven by a unit white noise vector w as in Eq. (4), the value of $\|T_{zw}\|_2^2$ is the asymptotic variance of the performance channel output:

$$\|T_{zw}\|_2^2 = \lim_{T\to\infty} \mathbb{E}\left\{\frac{1}{T}\int_0^T z(t)^T z(t)dt\right\} = \lim_{T\to\infty} \mathbb{E}\left\{\frac{1}{T}\int_0^T \|x_{1:4}(t)\|_2^2 + r^2\|u_e(t)\|_2^2 dt\right\} \tag{6}$$

Hence, the $\mathcal{H}_2$ norm provides a direct measure of the system output energy. The weight factor r in Eq. (6) decides a trade-off between the pure performance (i.e., $\|x_{1:4}\|_2^2$) and the muscle control effort (i.e., $\|u_e\|_2^2$). In general, the control effort can be reduced by increasing the weight factor r at the expense of increasing the pure performance-cost.

Now we introduce optimization techniques for synthesizing a fixed-structure neuromuscular controller with respect to the $\mathcal{H}_2$ performance-cost. The problem of synthesizing an optimal fixed-structure feedback controller K for the spine system in Eq. (4) can be formulated as the optimization over a set of bilinear matrix inequalities (BMIs). However, the optimization over a set of BMIs, which is nonconvex, is difficult to solve. On the other hand, several local search optimization algorithms have been proposed [26–28]. A straightforward local approach takes advantage of the fact that, by fixing a set of the bilinearly coupled variables, the BMI problem becomes a convex optimization problem in the remaining variables and vice versa. The algorithm then iterates among two LMI optimization problems. In each LMI problem, a set of bilinearly coupled variables is kept constant and the minimum is searched among their bilinear conjugates. This coordinate descent algorithm is effective and guarantees that the synthesized controller improves the performance as the number of iterations increases. However, it does not guarantee that it converges to a locally optimal solution for the originally formulated BMI problem. The recently developed PENBMI [29], which is a program package for solving optimization problems with quadratic objective and BMI constraints, guarantees the convergence to a critical point satisfying first-order Karush–Kuhn–Tucker (KKT) optimality conditions. However, the PENBMI package returns the optimal controller and cannot generate way points of controllers. The following gradient method with a smaller step size can also find a critical point.

The next theorem gives the gradient of the $\mathcal{H}_2$ cost function $J(K) := \|T_{zw}(K)\|_2^2$ [30].

THEOREM 1. *Let K be a stabilizing controller. Then the partial differential of J(K) with respect to K_{pq} is given as follows:*

$$\frac{\partial J(K)}{\partial K_{pq}} = 2\ \mathrm{tr}(MY)$$

$$M := (GB_u + C_z^T D_{zu} + C_y^T K^T D_{zu}^T D_{zu}) E_{pq} C_y \tag{7}$$

where $E_{pq} := \partial K / \partial K_{pq}$, i.e., E_{pq} is the matrix such that (p,q)th element is equal to 1 and the others are equal to 0, and G and Y are the solutions of the Lyapunov equations

$$A_{cl}^T G + G A_{cl} + C_{cl}^T C_{cl} = 0$$

and

Table 1 Experimentally determined (K_0) and optimized control gains (K_{opt1}, K_{opt2})

K_0	[109.9 33.6 61.3 53.8]
$K_{opt1}(r=0.001)$	[117.9 37.6 61.2 48.7]
$K_{opt2}(r=0.5)$	[88.6 28.6 24.5 13.3]

Table 2 $\mathcal{H}_2$ norms for the balancer

		$r=0.001$	$r=0.5$
$\|T_{zw}\|_2$	Initial	0.032333	0.28392
	Optimal	0.032048	0.24313
	Improvement	0.88%	14.37%
$\|T_{xw}\|_2$	Initial	0.032329	0.032329
	Optimal	0.032043	0.045506
	Improvement	0.88%	−40.76%
$\|T_{uw}\|_2$	Initial	0.56415	0.56415
	Optimal	0.58429	0.47766
	Improvement	−3.57%	15.33%

$$A_{cl}Y + YA_{cl}^T + B_wB_w^T = 0$$

respectively.

Using Eq. (7), the (p,q)th element of a descent direction ΔK can be easily obtained as

$$\Delta K_{pq} := -2\ \mathrm{tr}(MY) \tag{8}$$

Then, a gradient method for the $\mathcal{H}_2$ control problem can be summarized as follows [30].

1. [Initial K]: The initial controller is extracted from the individual. Set K^1 to the initial point. Also set $j=1$.
2. Get G^j and Y^j, which are the solutions of

$$A_{cl}^{jT}G^j + G^jA_{cl}^j + C_{cl}^{jT}C_{cl}^j = 0$$

and

$$A_{cl}^jY^j + Y^jA_{cl}^{jT} + B_w^jB_w^{jT} = 0$$

respectively, where

$$A_{cl}^j = A + B_uK^jC_y, \quad C_{cl}^j = C_z + D_{zu}K^jC_y$$

3. Calculate the partial derivative of $J(K)$ with respect to K_{pq} via Eq. (7) and define the descent direction ΔK via Eq. (8). If ΔK is a zero matrix, then the optimized gain $K_{opt}=K^j$. Otherwise, go to the next step.
4. Let $K^{j+1}=K^j+\epsilon^j\Delta K$, where $0<\epsilon^j<\bar{\epsilon}$ is a step size with an upper bound $\bar{\epsilon}$, which is the solution of

$$\min_{\epsilon}\|T_{zw}(K^j + \epsilon\Delta K)\|_2$$

Let $j=j+1$ and go to step 2.

The $\mathcal{H}_2$ performance norm condition alone may deteriorate the transient response of the closed-loop spine system. We can shape the transient response of the system by placing the poles at a region in the complex domain. Theorem 2 in Ref. [31] can be used to place the closed-loop poles into a predefined region in order to obtain satisfactory transient response.

4 An Illustrative Case Study

In this section, the proposed approach is applied to design the optimal neuromuscular controllers for an individual. Identified parameters were used to build the mathematical model of the spine system for the individual. Neuromuscular controllers were synthesized using the linearized spine system with approximated delays introduced in Sec. 2, while simulation results of the spine systems with synthesized controllers were obtained using the exact nonlinear spine system with delays. However, there was no noticeable difference between simulation results of exact and linearized systems.

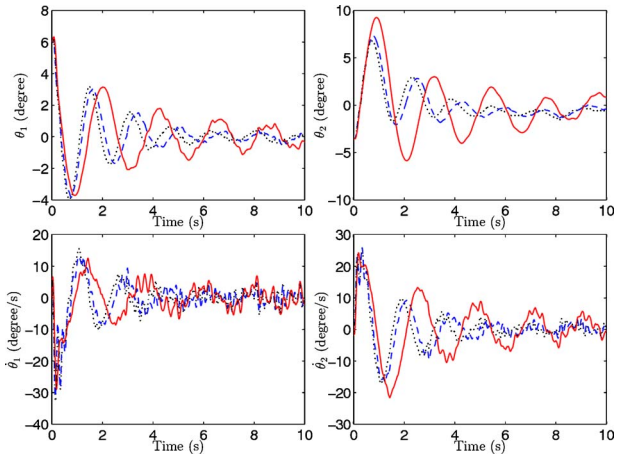

Fig. 6 Trajectories ($\theta_1, \theta_2, \dot{\theta}_1, \dot{\theta}_2$) from simulation studies with original gains (dotted lines), with $\mathcal{H}_2$ gains and $r=0.001$ (dashed lines), and with $\mathcal{H}_2$ gains and $r=0.5$ (solid lines)

Table 1 shows the identified original feedback gains along with the $\mathcal{H}_2$ optimized control gains for the subject using the above mentioned gradient method. The optimization time is less than 1 h making it appropriate for clinical treatment. The exactly same results were obtained by solving the optimization problem via PENBMI. Table 2 lists $\mathcal{H}_2$ norms of the following transfer functions:

(a) T_{zw}: from the input w to the total performance output z
(b) T_{xw}: from the input w to the pure performance output $x_{1:4}=[x_1,x_2,x_3,x_4]^T$
(c) T_{uw}: from the input w to the control effort u_e of the spine systems with experimentally determined initial gains and optimized control gains

Recall that the $\mathcal{H}_2$ norm of a transfer function is equivalent to the standard deviation of the steady-state output variable in our case.

In this section, we use the percentage improvement defined by the following formula:

$$\text{improvement} := \frac{\text{initial value} - \text{updated value}}{\text{initial value}} \times 100\%$$

Improvements in $\mathcal{H}_2$ norms of T_{zw}, T_{xw}, and T_{uw} are summarized in Table 2 under two different values for r defined in Eq. (6).

The simulated time responses using the optimized gains were compared with those using original gains. Let K_0, K_{opt1}, and K_{opt2} denote, respectively, the experimentally determined initial controller, the $\mathcal{H}_2$ controller optimized for $r=0.001$, and another $\mathcal{H}_2$ controller optimized for $r=0.5$. The trajectories of states $x_{1:4}=[\theta_1,\theta_2,\dot{\theta}_1,\dot{\theta}_2]^T$ and the corresponding control effort u_e under different controllers (K_0, K_{opt1}, and K_{opt2}) are illustrated, respectively, in Figs. 6 and 7.

In the case of $r=0.001$, the pure performance cost decreased slightly by 0.88% while the control effort cost increased by 3.57%. Hence, the pure performance was improved slightly at the expense of the control effort. Figure 8 shows the way points of optimized controller gains and their associated performance-cost values with respect to the number of iterations during the $\mathcal{H}_2$ optimization. Converged controller gains are listed in Table 1.

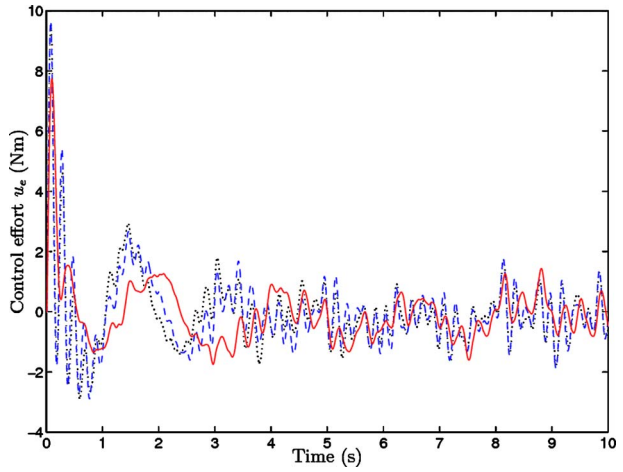

Fig. 7 Control efforts from simulation studies with original gains (dotted line), with $\mathcal{H}_2$ gains and r=0.001 (dashed line), and with $\mathcal{H}_2$ gains and r=0.5 (solid line)

Considering the small improvement (0.88%) and small changes between experimentally determined initial and optimized gains, we can infer that the subject may have optimized his gains according to this $\mathcal{H}_2$ cost function under r=0.001 defined in Eq. (6). In this case (r=0.001), the trajectories of states are represented by dashed lines in Fig. 6. The transient behavior of this spine system was similar to that of the initial system (in dotted lines). The increased variance of the control effort (in a dashed line) as compared with that of the original control effort (in a dotted line) can be observed in Fig. 7.

In the case of r=0.5, the control effort decreased significantly by 15.33% while the pure performance was impaired by 40.76%. Hence, the control effort cost was significantly improved at the expense of the pure performance-cost. In Fig. 9, it is straightforward to see that this optimization cost function decreased each of controller gains in order to save the control effort. Way points of optimized controller gains and their associated performance-cost values are also presented in Fig. 9. In this case (r=0.5), the trajectories of states are represented by the solid lines in Fig. 6. The transient behavior of this spine system was deteriorated as compared with that of the initial system (in dotted lines) in order to save control energy. The decreased variance of the control effort (in a solid line) as compared with that of the original control effort (in a dotted line) can be seen in Fig. 7.

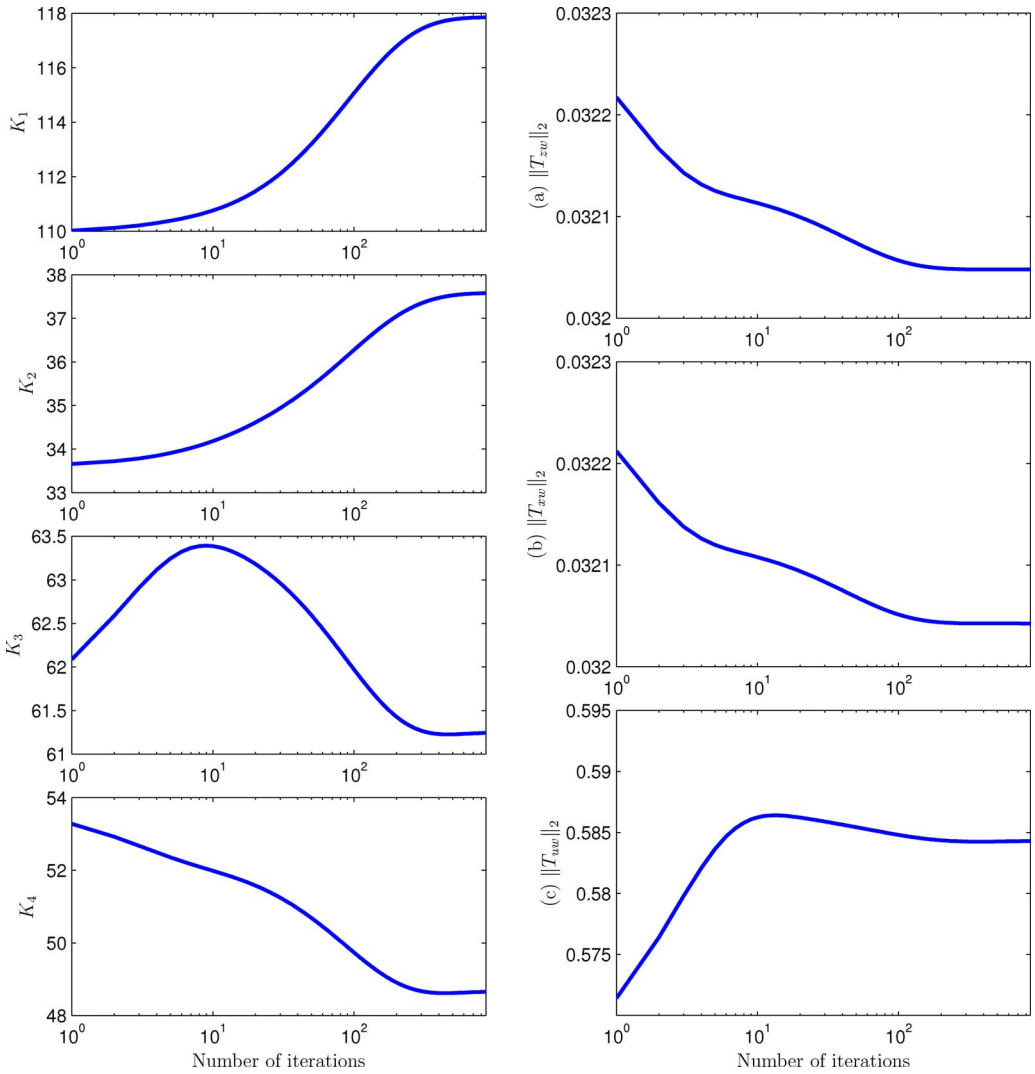

Fig. 8 Optimal control with r=0.001: way points of optimized gains and their associated $\mathcal{H}_2$ norms versus the number of iterations

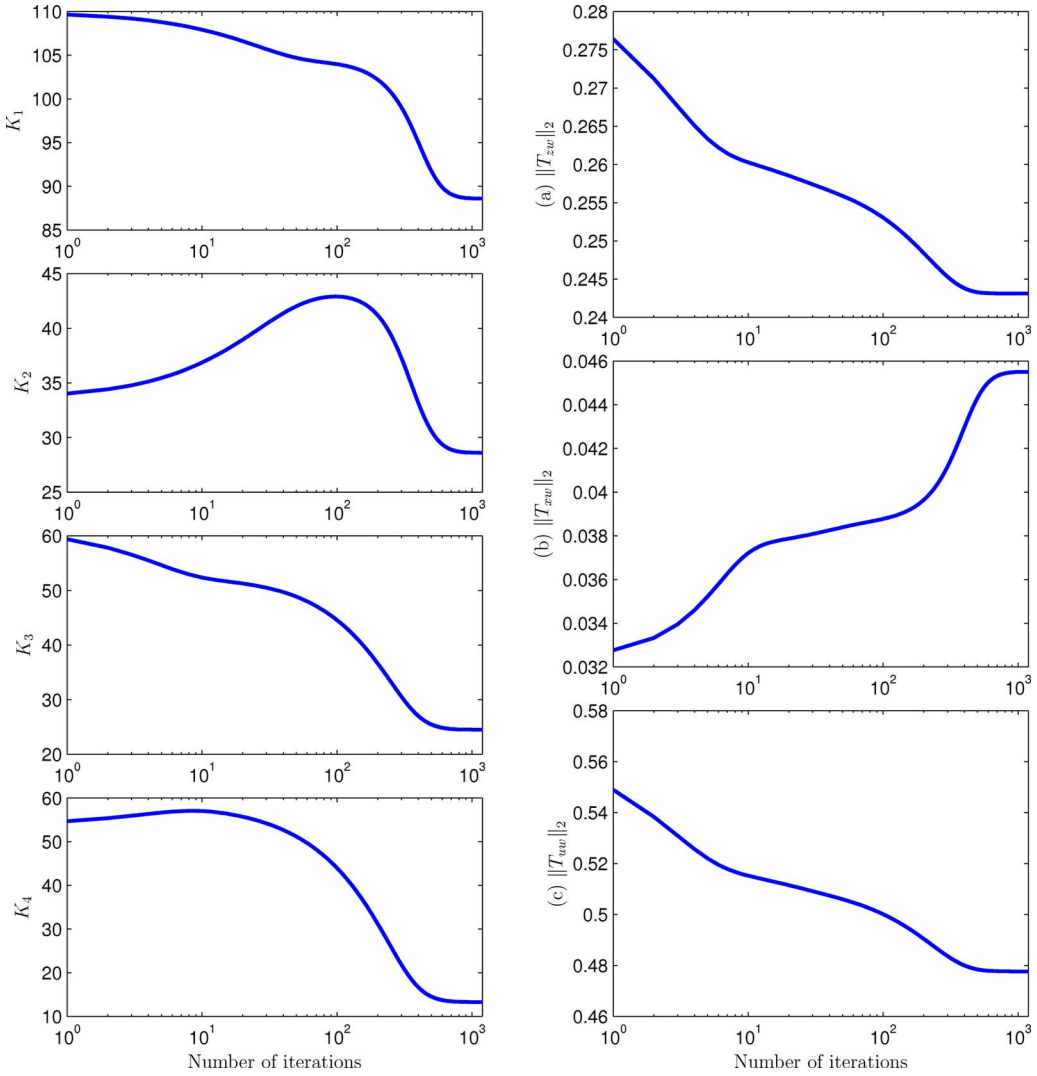

Fig. 9 Optimal control with r=0.5: way points of optimized gains and their associated $\mathcal{H}_2$ norms versus the number of iterations

5 The Robust Controllers

The spine system has to be modeled correctly and its parameters have to be estimated precisely. However, in practice, the obtained model and identified parameters are subject to modeling and estimation errors. For instance, in our seated balance task not all trunk rotation occurs in the lumbar region. Moreover, the parameters of the spine system can vary slightly in time, depending on the physiological conditions of the subject. Therefore, it is important to design robust controllers with respect to changes and uncertainty in the mathematical model of the actual spine system.

In this section, we investigate this issue of robustness by considering the following two scenarios. We consider the $\mathcal{H}_2$ controllers with r=0.001 and r=0.5 for the estimated time delay τ =0.01 s.

- *Scenario 1:* The true time delay was τ_1=0.0175 s, which was used to simulate the three nonlinear spine systems with K_0, K_{opt1}, and K_{opt2}, as shown in Fig. 10. In this scenario, the spine system with K_{opt1} became unstable while the other systems with K_0 and K_{opt2} were stable with respect to the equilibrium point.
- *Scenario 2:* The true time delay was τ_2=0.02 s, which was used to simulate the three spine systems with K_0, K_{opt1}, and K_{opt2}, as shown in Fig. 11. In this scenario, the systems with K_0 and K_{opt1} became unstable while the system with K_{opt2} was stable with respect to the equilibrium point.

In this simulation study, we can clearly see that the systems with K_0 and K_{opt1} that are highly optimized for the pure performance and so have rather aggressive high gains are very fragile and, therefore, are not robust with respect to changes in time delays. The mild control effort by K_{opt2} seems to make the spine system robust with respect to uncertain time delays. In classical control, it is well known that the combination of a high loop gain and long latencies of reflexes is prone to instability. This detrimental combination has been addressed in the context of sensory feedback in postural control [32,33]. The spine systems with aggressive gains K_0 and K_{opt1} are not robust and so K_0 and K_{opt1} are not recommendable for the patient. Perhaps, a rehabilitation therapy based on K_{opt2} is more appropriate for the patient.

This observation suggests the use of the robust control approach [17] to cope with uncertainty and time varying properties in the spine system.

6 Discussion

Using modern control theory, this paper presented methodology to evaluate the performance of a spine system and to synthesize optimal neuromuscular control. The robustness of the closed-loop

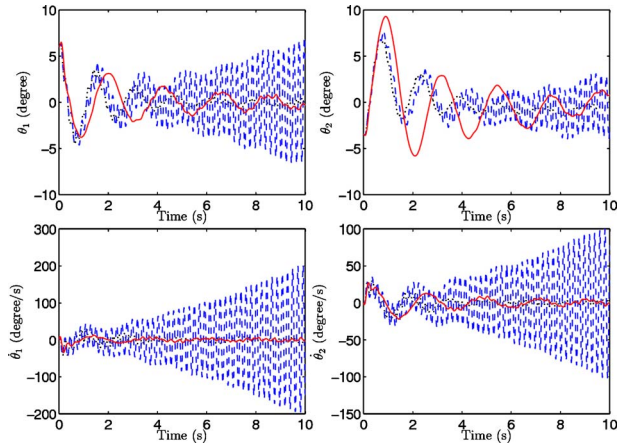

Fig. 10 The case of the true time delay $\tau_1=0.0175$ s: trajectories $(\theta_1, \theta_2, \dot{\theta}_1, \dot{\theta}_2)$ from simulation studies with original gains (dotted lines), with $\mathcal{H}_2$ gains and $r=0.001$ (dashed lines), and with $\mathcal{H}_2$ gains and $r=0.5$ (solid lines)

system with respect to time delays was analyzed. For a given specific task and a performance measure, we demonstrated how to synthesize way points of neuromuscular control gains, which can be used in rehabilitation planning. Specifically, we demonstrated the following.

- A performance-cost function can be designed to improve the performance of the spine system with respect to a critical task.
- Optimal gains for the chosen performance-cost function can be synthesized.
- A performance-cost function has to be designed to make the closed-loop system robust with respect to uncertainty in the spine model.

To improve our method further, we have to introduce (1) optimized parameter estimation techniques that minimize the estimation error and (2) the robust control [17] approach to cope with uncertainty and time varying properties in the spine system.

As mentioned earlier, the synthesized optimal gains could perhaps be used in the future for planning and guiding a low back rehabilitation program. $\mathcal{H}_2$ controller synthesis techniques introduced in Sec. 3 such as the gradient method produce way points of control gains and their associated performance-cost values. Way points of $\mathcal{H}_2$ control gains for the individual have been generated at each iteration step as a byproduct of the gradient method, as shown in Figs. 8 and 9. The set of identified control gains from the experiment was used as an initial point for the optimization. The overall performance-cost value $\|T_{zw}\|_2$ ($\mathcal{H}_2$ norm from w to z) for each of the way points decreases monotonically as the number of iterations increases (Figs. 8 and 9). Provided that the control gains of a patient can be modified using a similar method as in Refs. [34,35], way points of control gains from the initial point to the optimized final point (e.g., Figs. 8 and 9) can serve as a patient-specific table, which can be greatly exploited in rehabilitation. Thus an example of rehabilitation planning process would be as follows.

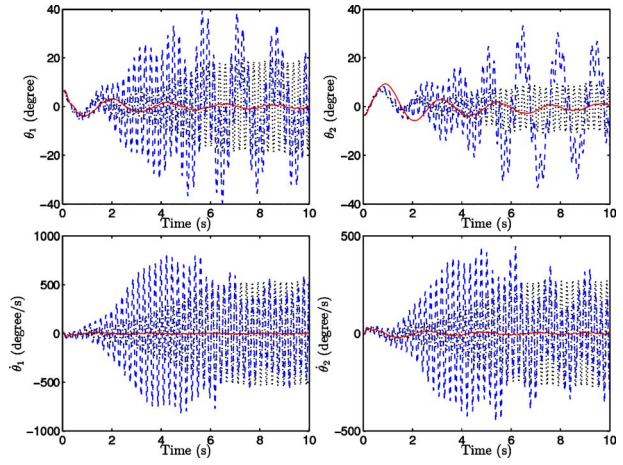

Fig. 11 The case of the true time delay $\tau_2=0.02$ s: Trajectories $(\theta_1, \theta_2, \dot{\theta}_1, \dot{\theta}_2)$ from simulation studies with original gains (dotted lines), with $\mathcal{H}_2$ gains and $r=0.001$ (dashed lines), and with $\mathcal{H}_2$ gains and $r=0.5$ (solid lines)

1. Choose a patient-specific critical task for which the spine system is to be optimized. In our example, the seated balance task was chosen.
2. Obtain the mathematical model of the critical task.
3. Collect experimental data for this critical task.
4. Measure the patient-specific anthropometric parameters and estimate control system parameters, such as initial neuromuscular control gains and time delays from the experimental data.
5. Choose a performance-cost function to be optimized and the necessary specifications (in time and/or frequency domain) by carefully considering patient's clinical presentation and the corresponding rehabilitation goals.
6. Generate the patient-specific control gain look-up table that consists of way points of the optimized control gains and their associated performance-cost values for the chosen performance-cost function in step 4 (e.g., Figs. 8 and 9).
7. Select target control gains from the patient-specific control gain look-up table considering associated performance-cost values.
8. Perform simulation study to evaluate the robustness of the closed-loop system with respect to uncertain parameters in the spine model. If the target control gains do not meet the robustness criterion, go to either step 4 or step 6 to select another set of target control gains.
9. Transform the patient's current control gains to the target control gains following a similar method as in Refs. [34,35]. During this step, the different target control gains can be selected (as in step 6) depending on the progress of rehabilitation. The goal of this final step is for the patient to attain the chosen target control gains at the end of the rehabilitation period.

These rehabilitation planning steps are summarized in the flowchart in Fig. 12. The basic principle of this approach is that gain adjustment comes from the central nervous system, which can be modified through rehabilitation and training. It should be also pointed out that the proposed rehabilitation approach is general and so can be applied to other neuromuscular and motor control impairments.

To implement the above framework, we need to develop rehabilitation modalities that are able to transform patient's current control gains to the target control gains that were synthesized using the presented method. Burdet and co-workers [34,35] used a robotic manipuladum with varying force fields to demonstrate that such a gain transformation is possible in the control of the upper extremity. Therefore, it is likely that control gains can be also modified in the trunk. However, a number of unknowns, specific to the spine and LBP, require extensive future research. We currently do not know what critical tasks should be optimized for the best rehabilitation results. We selected the seated balance exercise as an example because it emphasizes trunk muscles' contribution to postural control. Furthermore, patients with LBP perform significantly worse than healthy individuals in this task [15]. However, other tasks might be equally or more effective. Perhaps these

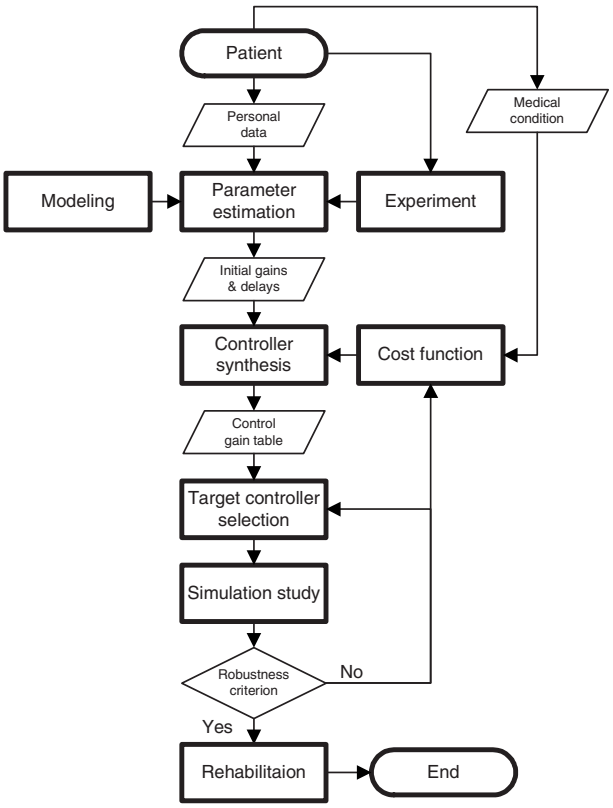

Fig. 12 The flowchart of the proposed rehabilitation planning

critical tasks should be patient specific and selected considering patient's occupation and activities of daily living.

Clinical guidelines regarding the selection of performance-cost functions to be optimized during the rehabilitation process need to be established. A performance-cost function, that best represents the goal of rehabilitation regarding transient or steady-state behaviors, has to be determined among different functions such as $\mathcal{H}_2$ and $\mathcal{H}_\infty$ norms [17]. Most likely multiobjective (or mixed) performance-cost functions [31] in the rehabilitation program will be required depending on the specific diagnoses. Furthermore, in choosing a performance-cost function in our case, the weight factor r on the control effort in Eq. (6) should be carefully selected based on the performance requirements and the patient's clinical presentation. For instance, in younger, more athletic patients with short neuromuscular delays, control can be more aggressive. In this patient population, there will be less concern with robustness issues from the combination of high feedback gains and delays, since delays are short. Whereas in an elderly patient with longer delays and diminished endurance, aggressive control could be problematic. Therefore, a high value for r can be chosen for an elderly patient to minimize the control effort at the cost of the pure performance with respect to the critical task. As discussed in Sec. 5, a good trade-off point between the pure performance and the control effort has to be chosen to make the closed-loop system efficient and robust with respect to the uncertain model parameters.

Finally, correct recommendations for the selection of specific target control gains must be formulated. Is it better to exercise patients with the final optimized gains as a target or to guide them by changing the gains slowly along the synthesized way points? The answers to these questions will require extensive future work that consists of a mixture of experimental and clinical trial research. Given the limited knowledge of clinicians in the area of modeling, an autonomous system may have to be developed. While the practical implementation of the presented rehabilitation program might still be some time away, the goal of this paper was to present a conceptual framework and to stimulate the necessary research in this area.

References

[1] Crisco, J., and Panjabi, M., 1992, "Euler Stability of the Human Ligamentous Lumbar Spine: Part I. Theory," Clin. Biomech. (Bristol, Avon), **7**, pp. 19–26.

[2] Reeves, N. P., Narendra, K., and Cholewicki, J., 2007, "Spine Stability: The Six Blind Men and the Elephant," Clin. Biomech. (Bristol, Avon), **22**(3), pp. 266–274.

[3] Marras, W. S., Davis, K. G., and Maronitis, A. B., 2001, "A Non-MVC EMG Normalization Technique for the Trunk Musculature: Part 2. Validation and Use to Predict Spinal Loads," Journal of Electromyography and Kinesiology, **11**(1), pp. 11–18.

[4] Larivière, C., Gagnon, D., and Loisel, P., 2000, "The Comparison of Trunk Muscles EMG Activation Between Subjects With and Without Chronic Low Back Pain During Flexionextension and Lateral Bending Tasks," J. Electromyogr Kinesiol, **10**(2), pp. 79–91.

[5] van Dieën, J., Cholewicki, J., and Radebold, A., 2003, "Trunk Muscle Recruitment Patterns in Patients With Low Back Pain Enhance the Stability of the Lumbar Spine," Spine, **28**(8), pp. 834–841.

[6] Hodges, P., Moseley, G., Gabrielsson, A., and Gandevia, S., 2003, "Experimental Muscle Pain Changes Feedforward Postural Responses of the Trunk Muscles," Exp. Brain Res., **151**(2), pp. 262–271.

[7] Reeves, N., Everding, V., Cholewicki, J., and Morrisette, D., 2006, "The Effects of Trunk Stiffness on Postural Control During Unstable Seated Balance," Exp. Brain Res., **174**(4), pp. 694–700.

[8] Stein, R., Hunter, I., Lafontaine, S., and Jones, L., 1995, "Analysis of Short-Latency Reflexes in Human Elbow Flexor Muscles," J. Neurophysiol., **73**(5), pp. 1900–1911.

[9] Magnusson, M., Aleksiev, A., Wilder, D., Pope, M., Spratt, K., Lee, S., Goel, V., and Weinstein, J., 1996, "Unexpected Load and Asymmetric Posture as Etiologic Factors in Low Back Pain," Eur. Spine J., **5**, pp. 23–35.

[10] Radebold, A., Cholewicki, J., Panjabi, M., and Patel, T., 2000, "Muscle Response Pattern to Sudden Trunk Loading in Healthy Individuals and in Patients With Chronic Low Back Pain," Spine, **25**(8), pp. 947–954.

[11] Reeves, N., Cholewicki, J., and Milner, T., 2005, "Muscle Reflex Classification of Low-Back Pain," J. Electromyogr Kinesiol, **15**(1), pp. 53–60.

[12] Thomas, J., France, C., Sha, D., Vander Wiele, N., Moenter, S., and Swank, K., 2007, "The Effect of Chronic Low Back Pain on Trunk Muscle Activations in Target Reaching Movements With Various Loads," Spine, **32**(26), pp. E801–E808.

[13] Mientjes, M. I., and Frank, J. S., 1999, "Balance in Chronic Low Back Pain Patients Compared to Healthy People Under Various Conditions in Upright Standing," Clin. Biomech. (Bristol, Avon), **14**(10), pp. 710–716.

[14] Luoto, S., Aalto, H., Taimela, S., Hurri, H., Pyykko, I., and Alaranta, H., 1998, "One-Footed and Externally Disturbed Two-Footed Postural Control in Patients With Chronic Low Back Pain and Healthy Control Subjects: A Controlled Study With Follow-Up," Spine, **23**(19), pp. 2081–2089.

[15] Radebold, A., Cholewicki, J., Polzhofer, G., and Greene, H., 2001, "Impaired Postural Control of the Lumbar Spine Is Associated With Delayed Muscle Response Times in Patients With Chronic Idiopathic Low Back Pain," Spine, **26**(7), pp. 724–730.

[16] Hodges, P., van den Hoorn, W., Dawson, A., and Cholewicki, J., 2009, "Changes in the Mechanical Properties of the Trunk in Low Back Pain May Be Associated With Recurrence," J. Biomech., **42**(1), pp. 61–66.

[17] Zhou, K., Doyle, J., and Glover, K., 1996, *Robust and Optimal Control*, Prentice-Hall, Upper Saddle River, NJ.

[18] Boyd, S., 1994, *Linear Matrix Inequalities in System and Control Theory*, Society for Industrial Mathematics & Applied Mathematics (SIAM).

[19] Dullerud, G., and Paganini, F., 2000, *A Course in Robust Control Theory: A Convex Approach*, Springer, New York.

[20] Silfies, S. P., Cholewicki, J., Reeves, N. P., and Greene, H. S., 2007, "Lumbar Position Sense and the Risk of Low Back Injuries in College Athletes: A Prospective Cohort Study," BMC Musculoskelet. Disord., **8**(1), pp. 129.

[21] Reeves, N., Cholewicki, J., Milner, T., and Lee, A., 2008, "Trunk Antagonist Coactivation Is Associated With Impaired Neuromuscular Performance," Exp. Brain Res., **188**(3), pp. 457–463.

[22] van der Kooij, H., van Asseldonk, E., and van der Helm, F., 2005, "Comparison of Different Methods to Identify and Quantify Balance Control," J. Neurosci. Methods, **145**(1–2), pp. 175–203.

[23] Cordo, P., Inglis, J., Verschueren, S., Collins, J., Merfeld, D., Rosenblum, S., Buckley, S., and Moss, F., 1996, "Noise in Human Muscle Spindles," Nature (London), **383**(6603), pp. 769–770.

[24] Reeves, N., Cholewicki, J., and Narendra, K., 2009, "Effects of Reflex Delays on Postural Control During Unstable Seated Balance," J. Biomech., **42**(2), pp. 164–70.

[25] Prochazka, A., Gillard, D., and Bennett, D., 1997, "Implications of Positive Feedback in the Control of Movement," J. Neurophysiol., **77**(6), pp. 3237–3251.

[26] El Ghaoui, L., and Balakrishnan, V., 1994, "Synthesis of Fixed-Structure Controllers Via Numerical Optimization," Proceedings of the 33rd IEEE Conference on Decision and Control, Vol. 3.

[27] Fukuda, M., and Kojima, M., 2001, "Branch-and-Cut Algorithms for the Bilinear Matrix Inequality Eigenvalue Problem," Comput. Optim. Appl., **19**(1),

pp. 79–105.
[28] Iwasaki, T., 1999, "The Dual Iteration for Fixed-Order Control," IEEE Trans. Autom. Control, **44**(4), pp. 783–788.
[29] Kocvara, M., and Stingl, M., 2006, PENBMI User's Guide (Version 2.1), PENOPT GbR, Germany.
[30] Kami, Y., and Nobuyama, E., 2008, "A Gradient Method for the Static Output Feedback Mixed H_2/H_∞ Control," Proceedings of the 17th World Congress, The International Federation of Automatic Control, Seoul, Korea, pp. 7838–7842.
[31] Scherer, C., Gahinet, P., and Chilali, M., 1997, "Multiobjective Output-Feedback Control Via LMI Optimization," IEEE Trans. Autom. Control, **42**(7), pp. 896–911.
[32] Fitzpatrick, R., Burke, D., and Gandevia, S., 1996, "Loop Gain of Reflexes Controlling Human Standing Measured With the Use of Postural and Vestibular Disturbances," J. Neurophysiol., **76**(6), pp. 3994–4008.
[33] Rack, P., Ross, H., and Thilmann, A., 1984, "The Ankle Stretch Reflexes in Normal and Spastic Subjects: The Response to Sinusoidal Movement," Brain, **107**(2), pp. 637–654.
[34] Burdet, E., Osu, R., Franklin, D., Milner, T., and Kawato, M., 2001, "The Central Nervous System Stabilizes Unstable Dynamics by Learning Optimal Impedance," Nature (London), **414**(6862), pp. 446–449.
[35] Franklin, D., Osu, R., Burdet, E., Kawato, M., and Milner, T., 2003, "Adaptation to Stable and Unstable Dynamics Achieved by Combined Impedance Control and Inverse Dynamics Model," J. Neurophysiol., **90**(5), pp. 3270–3282.